

# Photoactivable glycolipid antigens generate stable conjugates with CD1d for invariant Natural Killer T cell activation

Kharkwal, Shalu Sharma; Veerapen, Natacha; Jervis, Peter; Bhowruth, Veemal; Besra, Amareeta K; North, Simon J; Haslam, Stuart M; Dell, Anne; Hobrath, Judith; Quaid, Padraic; Moynihan, Patrick; Cox, Liam Robert; Kharkwal, Himanshu; Zauderer, Maurice; Besra, Gurdyal S; Porcelli, Steven A

DOI:

[10.1021/acs.bioconjchem.8b00484](https://doi.org/10.1021/acs.bioconjchem.8b00484)

License:

Other (please specify with Rights Statement)

*Document Version*

Peer reviewed version

*Citation for published version (Harvard):*

Kharkwal, SS, Veerapen, N, Jervis, P, Bhowruth, V, Besra, AK, North, SJ, Haslam, SM, Dell, A, Hobrath, J, Quaid, P, Moynihan, P, Cox, LR, Kharkwal, H, Zauderer, M, Besra, GS & Porcelli, SA 2018, 'Photoactivable glycolipid antigens generate stable conjugates with CD1d for invariant Natural Killer T cell activation', *Bioconjugate Chemistry*. <https://doi.org/10.1021/acs.bioconjchem.8b00484>

[Link to publication on Research at Birmingham portal](#)

**Publisher Rights Statement:**

Checked for eligibility: 14/08/2018

This is the accepted manuscript for a forthcoming publication in *Bioconjugate Chemistry*.

**General rights**

Unless a licence is specified above, all rights (including copyright and moral rights) in this document are retained by the authors and/or the copyright holders. The express permission of the copyright holder must be obtained for any use of this material other than for purposes permitted by law.

- Users may freely distribute the URL that is used to identify this publication.
- Users may download and/or print one copy of the publication from the University of Birmingham research portal for the purpose of private study or non-commercial research.
- User may use extracts from the document in line with the concept of 'fair dealing' under the Copyright, Designs and Patents Act 1988 (?)
- Users may not further distribute the material nor use it for the purposes of commercial gain.

Where a licence is displayed above, please note the terms and conditions of the licence govern your use of this document.

When citing, please reference the published version.

**Take down policy**

While the University of Birmingham exercises care and attention in making items available there are rare occasions when an item has been uploaded in error or has been deemed to be commercially or otherwise sensitive.

If you believe that this is the case for this document, please contact [UBIRA@lists.bham.ac.uk](mailto:UBIRA@lists.bham.ac.uk) providing details and we will remove access to the work immediately and investigate.

1  
2  
3 **1 Photoactivable glycolipid antigens generate stable conjugates with**  
4  
5  
6 **2 CD1d for invariant Natural Killer T cell activation**  
7  
8  
9 **3**

10  
11 4 Natacha Veerapen<sup>1#</sup>, Shalu Sharma Kharkwal<sup>3#</sup>, Peter Jervis<sup>1</sup>, Veemal Bhowruth<sup>1</sup>,  
12  
13 5 Amareeta K. Besra<sup>1</sup>, Simon J. North<sup>6</sup>, Stuart M. Haslam<sup>6</sup>, Anne Dell<sup>6</sup>, Judith Hobrath<sup>7</sup>,  
14  
15 6 Padraic J. Quaid<sup>1</sup>, Patrick J. Moynihan<sup>1</sup>, Liam R. Cox<sup>2</sup>, Himanshu Kharkwal<sup>4</sup>, Maurice  
16  
17 7 Zauderer<sup>8</sup>, Gurdial S. Besra<sup>1\*</sup>, Steven A. Porcelli.<sup>3,5\*</sup>  
18  
19  
20 8

21  
22 9 <sup>1</sup>School of Biosciences, and <sup>2</sup>School of Chemistry, University of Birmingham,  
23  
24 10 Edgbaston, Birmingham, B15 2TT, United Kingdom

25  
26  
27 11 <sup>3</sup>Department of Microbiology and Immunology, <sup>4</sup>Department of Developmental and  
28  
29 12 Molecular Biology, and <sup>5</sup>Department of Medicine, Albert Einstein College of Medicine,  
30  
31 13 Bronx, NY, 10461, USA

32  
33  
34 14 <sup>6</sup>Department of Life Sciences, Faculty of Natural Sciences, Imperial College  
35  
36 15 London, South Kensington Campus, London, SW7 2AZ, UK

37  
38 16 <sup>7</sup>Drug Discovery Unit, College of Life Sciences, University of Dundee, Dow Street  
39  
40  
41 17 Dundee, DD1 5EH, Scotland, UK

42  
43 18 <sup>8</sup>Vaccinex Inc., 1895 Mount Hope Avenue, Rochester, NY 14620, USA  
44  
45  
46 19

47  
48 20 #These authors contributed equally to this manuscript  
49

50 21 \*Joint corresponding authors  
51  
52  
53 22

1  
2  
3 **1 Correspondence to:**  
4

5  
6 **2 Steven A. Porcelli, MD**  
7

8  
9 **3 Department of Microbiology and Immunology**  
10

11  
12 **4 Forchheimer Building, Room 416**  
13

14  
15 **5 Albert Einstein College of Medicine**  
16

17  
18 **6 1300 Morris Park Avenue, Bronx, NY 10461**  
19

20  
21 **7 Phone: 718-430-3228. Fax: 718-430-8711**  
22

23  
24 **8 E-mail: [steven.porcelli@einstein.yu.edu](mailto:steven.porcelli@einstein.yu.edu)**  
25

26  
27  
28 **9**  
29

30  
31 **10 Gurdyal S. Besra**  
32

33  
34 **11 School of Biosciences**  
35

36  
37 **12 University of Birmingham**  
38

39  
40 **13 Edgbaston, Birmingham B15 2TT, UK**  
41

42  
43 **14 Phone: +00 44 121 415 8125. Fax: +00 44 121 414 5925**  
44

45  
46 **15 E-mail: [g.besra@bham.ac.uk](mailto:g.besra@bham.ac.uk)**  
47

48  
49  
50 **16**  
51

52  
53  
54 **17**  
55

## 1 **Abstract**

2  
3  
4  
5  
6 2 Activation of invariant natural killer T lymphocytes (iNKT cells) by  $\alpha$ -galactosylceramide  
7  
8 3 ( $\alpha$ -GC) elicits a range of pro-inflammatory or anti-inflammatory immune responses. We  
9  
10 4 report the synthesis and characterization of a series of  $\alpha$ -GC analogues with acyl chains  
11  
12 5 of varying length and a terminal benzophenone. These bound efficiently to the  
13  
14 6 glycolipid antigen presenting protein CD1d, and upon photoactivation formed stable  
15  
16 7 CD1d-glycolipid covalent conjugates. Conjugates of benzophenone  $\alpha$ -GCs with soluble  
17  
18 8 or cell bound CD1d proteins retained potent iNKT cell activating properties, with biologic  
19  
20 9 effects that were modulated by acyl chain length and the resulting affinities of  
21  
22 10 conjugates for iNKT cell antigen receptors. Analysis by mass spectrometry identified a  
23  
24 11 unique covalent attachment site for the glycolipid ligands in the hydrophobic ligand  
25  
26 12 binding pocket of CD1d. The creation of covalent conjugates of CD1d with  $\alpha$ -GC  
27  
28 13 provides a new tool for probing the biology of glycolipid antigen presentation, as well as  
29  
30 14 opportunities for developing effective immunotherapeutics.  
31  
32  
33  
34  
35  
36  
37  
38  
39

## 40 **Keywords**

41  
42  
43 17 CD1d,  $\alpha$ -galactosylceramide, benzophenone, invariant Natural Killer T cells  
44  
45  
46  
47  
48  
49  
50  
51  
52  
53  
54  
55  
56  
57  
58  
59  
60

## 1 Introduction

2 Invariant Natural Killer T (iNKT) cells are a prominent subset of unconventional T cells  
3 that bridge innate and adaptive immunity to contribute to a wide range of immune  
4 responses.<sup>1</sup> They recognize and respond to glycolipid antigens presented by CD1d, a  
5 membrane protein specialized for binding and presentation of lipid antigens.<sup>2</sup> The most  
6 extensively studied CD1d-presented glycolipid antigens are synthetic forms of  $\alpha$ -  
7 galactosylceramide ( $\alpha$ -GC), which potently stimulate iNKT cell proliferation, expansion  
8 and cytokine secretion.<sup>3</sup> In mice, various structural analogues of  $\alpha$ -GC have shown  
9 impressive anti-cancer effects<sup>4</sup>, as well as a broad range of activities in models of  
10 infection, vaccination, autoimmunity and inflammatory diseases.<sup>5</sup> Thus, there has  
11 been increasing interest in using  $\alpha$ -GC analogues to develop new approaches to  
12 vaccination or immunotherapy.<sup>4c, 6</sup>

13 Despite the potent immune activating properties of  $\alpha$ -GC and the  
14 conservation of a CD1d-restricted iNKT cell subset in humans, there has been  
15 limited success so far in translating iNKT cell-based approaches into clinical  
16 applications. This may reflect problems with systemic delivery of glycolipid agonists,  
17 which leads to their uptake and presentation by a wide range of cell types and the  
18 stimulation of unpredictable or antagonistic immune responses.<sup>6a, 7</sup>

19 Several approaches to overcoming these problems have been developed that  
20 involve delivery of  $\alpha$ -GC by antigen presenting cells (APCs) or soluble recombinant  
21 CD1d proteins loaded *ex vivo* with the glycolipid.<sup>8</sup> These approaches have shown  
22 potential to stimulate more effective antitumor responses compared to injections of  
23 free glycolipids in mouse models, as well as promising preliminary results in

1 preclinical and clinical studies.<sup>4c, 6a, 8c, 8d, 9</sup> Also of note is the apparent ability of  
2 these methods to induce substantial iNKT cell activation while triggering less of the  
3 long-term unresponsiveness (anergy) or depletion of iNKT cells that has been a  
4 problem with injections of free glycolipids.<sup>10</sup>

5 However, a potential limitation is presented by the readily reversible binding  
6 of glycolipid ligands to CD1d, which is mediated by noncovalent hydrophobic and  
7 hydrogen bonding interactions.<sup>2</sup> Rapid dissociation has been reported to result in  
8 half-lives for  $\alpha$ GC-CD1d complexes in some *in vitro* studies as short as a few  
9 minutes or less, which may be further reduced *in vivo* by the presence of lipid  
10 exchange and binding proteins.<sup>11</sup> The relatively short half-life and instability of such  
11 complexes limits the duration and potency of their desirable biologic effects, and the  
12 release of free glycolipids *in vivo* may contribute to unwanted effects such as iNKT  
13 cell anergy or toxicities including liver damage or sensitization to endotoxic shock.<sup>12</sup>  
14 Thus, the relative instability of  $\alpha$ GC-CD1d complexes remains a suboptimal feature  
15 in approaches that involve *ex vivo* loading of cells or CD1d proteins with glycolipids,  
16 and can compromise the efficacy and precision of such controlled delivery methods.

17 In the current study, we have developed an approach to circumvent the  
18 problem of glycolipid dissociation from CD1d by the use of photoactivatable forms  
19 of  $\alpha$ -GC to create covalently stabilized and highly active  $\alpha$ GC-CD1d conjugates. A  
20 series of analogues of  $\alpha$ -GC containing a benzophenone group at the terminus of  
21 their N-acyl chains was synthesized and optimized for iNKT cell stimulating activity.  
22 Controlled exposure to UV irradiation generated stable covalent conjugates of these  
23 glycolipids with CD1d, and these retained their ability to potently stimulate iNKT

1 cells *in vitro* and *in vivo* in mice. Specific immunologic properties such as cytokine  
2 production could be modulated by variations in the size of the aliphatic chain  
3 bearing the benzophenone group, which was correlated with the affinity of the  
4 conjugates for the antigen receptors of iNKT cells. Mass spectrometry identified a  
5 unique site for covalent bond formation in the CD1d protein, enabling detailed  
6 modeling of the structure of the stable conjugates. The development of controlled  
7 covalent bond formation for stabilization of  $\alpha$ GC-CD1d conjugates provides a new  
8 tool for the study of glycolipid antigen presentation, and also forms the basis for  
9 improving immunotherapies based on the targeted delivery of iNKT cell activators.

10

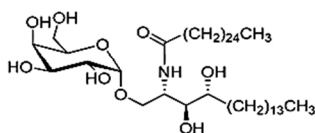
## 11 **Results**

### 12 **Synthesis of BPGCs**

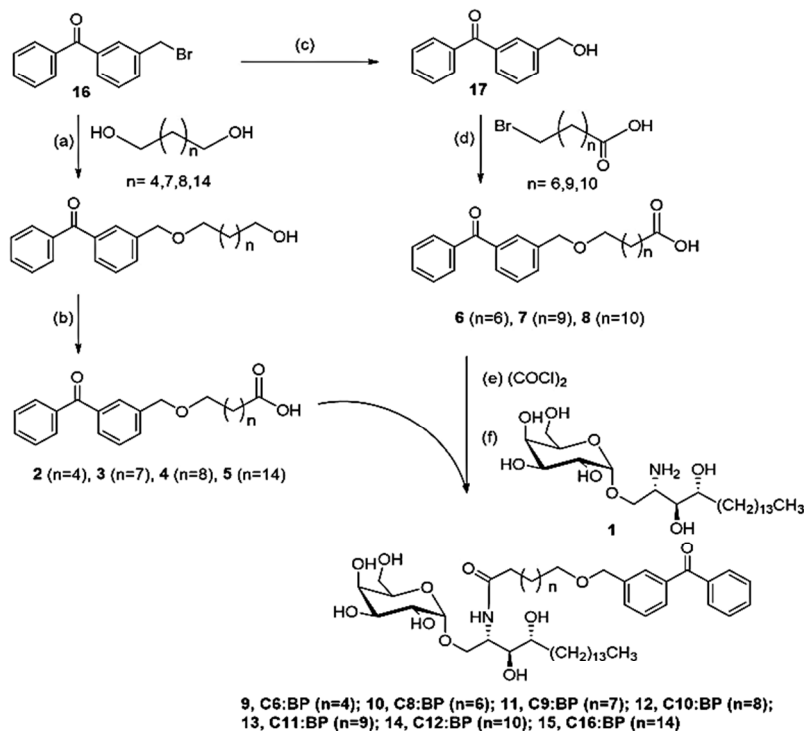
13 Extensive previous work has shown that many modifications of the fatty acyl chain of  
14  $\alpha$ -GC can be tolerated without disruption of glycolipid binding to CD1d or loss of iNKT  
15 cell stimulating activity<sup>3</sup>, consistent with the large volume of the hydrophobic ligand  
16 binding site of CD1d.<sup>2, 13</sup> Thus, we developed a synthetic strategy for introduction of a  
17 photoactivatable moiety on the acyl chain terminus of  $\alpha$ -GC to enable the controlled  
18 formation of a covalent bond between the glycolipid and the CD1d protein (**Fig. 1**). The  
19 benzophenone group was chosen as it can be activated by UV irradiation to give the  
20 corresponding benzhydryl biradical, which we postulated would react with a proximal  
21 C-H bond present in the CD1d protein to form a permanent covalent bond. A group of  
22 benzophenone-containing derivatives of  $\alpha$ -GC (BPGCs) bearing acyl chains of various  
23 lengths (compounds **9-15**) were synthesized to determine which would optimally

1 associate with CD1d and effectively activate iNKT cells. Based on the resemblance of  
 2 benzophenone to a C10 isoprene unit, we synthesized a range of BPGCs which mimic  
 3 *N*-acyl chain lengths from C16 (C6:BP (**9**)) to C26 (C16:BP (**15**)), thus spanning the  
 4 range found in most highly active  $\alpha$ -GC analogues.<sup>3</sup> These compounds were readily  
 5 prepared via acylation of the parent compound **1** with carboxylic acids (**2-8**), following  
 6 their conversion to the corresponding acid chlorides using oxalyl chloride. Ensuing  
 7 acylation of the amine **1** in a 1:1 mixture of THF and saturated sodium acetate solution  
 8 afforded the benzophenone-derivatised glycosphingolipids (BPGCs) **9-15** (Fig. 1).

a



b



9



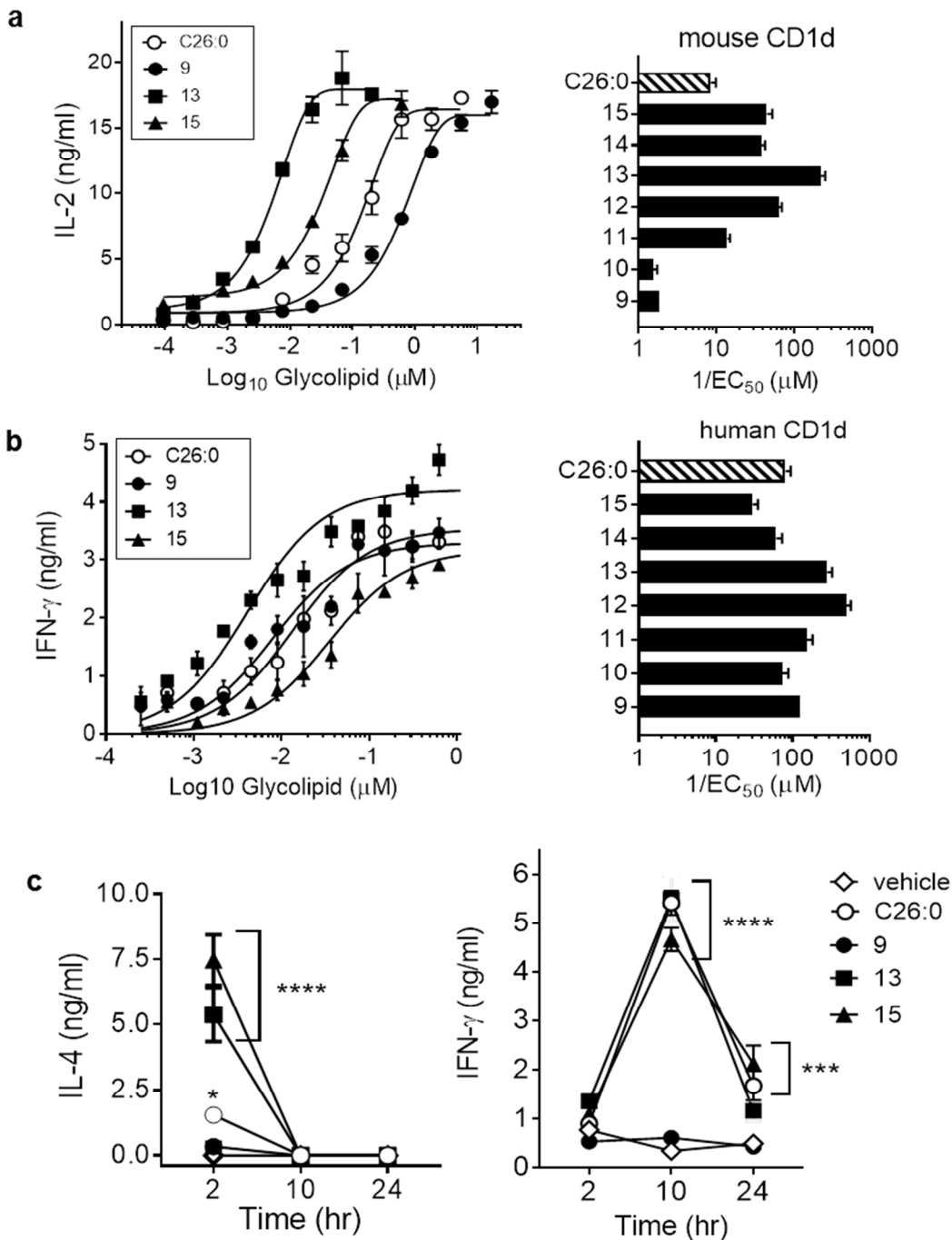
**Figure 1: Synthesis of BPGCs.** (a) Structure of the prototypical iNKT cell activating glycolipid,  $\alpha$ -GC C26:0. (b) General scheme for synthesis of BPGCs with acyl group spacers of varying length (compounds **9 – 15**). (a) NaH, DMF, 0 °C to rt; (b) PDC, wet THF, rt; (c) CaCO<sub>3</sub>, THF, H<sub>2</sub>O, 100 °C, 12 h; (d) NaH, DMF, 0 °C to rt; (e) (COCl)<sub>2</sub>, 60 °C, 2 h; (f) NaOAc, THF, rt, 12 h. Incorporation of the benzophenone group into carboxylic acids was accomplished through the use of a flexible ether linkage to allow rotational freedom and optimal orientation of the aromatic group in the CD1d ligand-binding pocket. To synthesize carboxylic acids (**2-8**), we used a versatile strategy involving an S<sub>N</sub>2 displacement of a bromide using various diols and 3-(bromomethyl)benzophenone (**16**) or through a variety of bromocarboxylic acids by 3-(hydroxymethyl)benzophenone (**17**). The monoalkylation of the diols with 3-(bromomethyl)benzophenone (**16**), which was obtained using published procedures<sup>14</sup>, was achieved in reasonable yields by using the diols in excess. Oxidation of the corresponding alcohols to the acids with pyridinium dichromate (PDC) was sluggish and only afforded compounds **2-5** in average yields. In contrast, alkylation of the alcohol **17** with the bromocarboxylic acids in DMF and sodium hydride as base proceeded smoothly to afford the desired carboxylic acids **6-8** in quantitative yields (see Supplemental Information for further details of synthesis and characterization).

### Stimulation of iNKT cells by BPGC analogs

A variety of *in vitro* biological assays were performed to assess the iNKT cell activating properties of the BPGCs upon presentation by CD1d, and to determine the effect of the varying acyl chain lengths and the presence of a bulky terminal benzophenone group on their biologic activities. A standard assay using co-culture of mouse bone marrow-derived dendritic cells (BMDCs) and a murine iNKT cell hybridoma was used to assess the activity and relative potencies of BPGCs (**Fig. 2a**).<sup>15</sup> This showed significant iNKT cell stimulating activity for all BPGCs tested, with a substantial impact of the length of fatty acyl chain. Optimal iNKT stimulation in the mouse cell culture system was

1  
2  
3 1 achieved with **13**, which along with several other BPGCs was significantly more potent  
4  
5 2 than the standard  $\alpha$ -GC (C26:0), which is generally considered a highly potent iNKT cell  
6  
7 3 activator both *in vitro* and *in vivo*.<sup>4a, 15</sup> A similar *in vitro* analysis was carried out using a  
8  
9 4 canonical human iNKT cell clone co-cultured with HeLa cells transfected to express  
10  
11 5 human CD1d (**Fig. 2b**).<sup>16</sup> This also revealed strong activity of BPGCs as measured by  
12  
13 6 IFN- $\gamma$  secretion, which was similar to or greater than that stimulated by C26:0. As for  
14  
15 7 the mouse culture system, compounds **12** and **13** showed the greatest potency in this  
16  
17 8 assay, although length of the fatty acyl tail had much less apparent impact in the human  
18  
19 9 system.

20  
21  
22  
23  
24 10 To directly assess activity *in vivo*, we analyzed serum cytokine levels following  
25  
26 11 intravenous injection of selected BPGCs. For this analysis, we tested **9** which was a  
27  
28 12 relatively weak activator of murine iNKT cells *in vitro*, and **13** and **15** which were more  
29  
30 13 potent than C26:0 in both mouse and human cell culture assays. Mice were injected  
31  
32 14 with 4 nmoles of each glycolipid and bled after 2, 10 and 24 hours to quantitate serum  
33  
34 15 IFN- $\gamma$  and IL-4, as previously described.<sup>15</sup> Significant levels above baseline for serum  
35  
36 16 IL-4 were detected with **13** and **15** at two hours, which declined to undetectable levels  
37  
38 17 by 10 hours (**Fig. 2c**). The IL-4 levels were several fold higher for **13** and **15** compared  
39  
40 18 to C26:0, indicating a rapid and powerful activation of iNKT cells. Consistent with this,  
41  
42 19 IFN- $\gamma$  levels showed a sustained rise with **13** and **15** with a peak at 10 hours that closely  
43  
44 20 resembled the response to C26:0, while **9** did not stimulate detectable levels above  
45  
46 21 background for either cytokine tested. Thus, BPGCs retained their iNKT cell activating  
47  
48 22 properties *in vivo*, and the potencies of different analogues varied depending on the  
49  
50 23 length of their acyl chains.



1  
2  
3  
4  
5  
6  
7  
8  
9  
10  
11  
12  
13  
14  
15  
16  
17  
18  
19  
20  
21  
22  
23  
24  
25  
26  
27  
28  
29  
30  
31  
32  
33  
34  
35  
36  
37  
38  
39  
40  
41  
42  
43  
44  
45  
46  
47  
48  
49  
50  
51  
52  
53  
54  
55  
56  
57  
58  
59  
60

**Figure 2: iNKT stimulatory activity of BPGCs.** (a) Responses of mouse iNKT cell hybridoma DN3A4-1.2 cultured with bone marrow derived dendritic cells from C57BL/6 mice and the indicated concentrations of BPGCs or  $\alpha$ -GC C26:0. IL-2 secretion was measured in supernatants after 18 hours of culture. Representative dose-response curves are shown on the left for three of the seven BPGCs and standard  $\alpha$ -GC C26:0.

1  
2  
3 1 Concentrations stimulating 50% of the maximum response ( $EC_{50}$ ) were determined for  
4 each glycolipid, and reciprocal values are plotted on the right. (b) Similar analysis as in  
5 2 (a) except using human iNKT clone HDE3 and HeLa cells expressing human CD1d with  
6 3 measurement of secreted IFN $\gamma$  as the readout for activation. (c) *In vivo* activities of **9**,  
7 4 **13** and **15** were determined by quantitating serum IL-4 and IFN- $\gamma$  2, 10 and 24 hours  
8 5 post glycolipid injection. Peak values for serum IL4 (left) and IFN- $\gamma$  (right) were found at  
9 6 2 and 10 hours respectively.

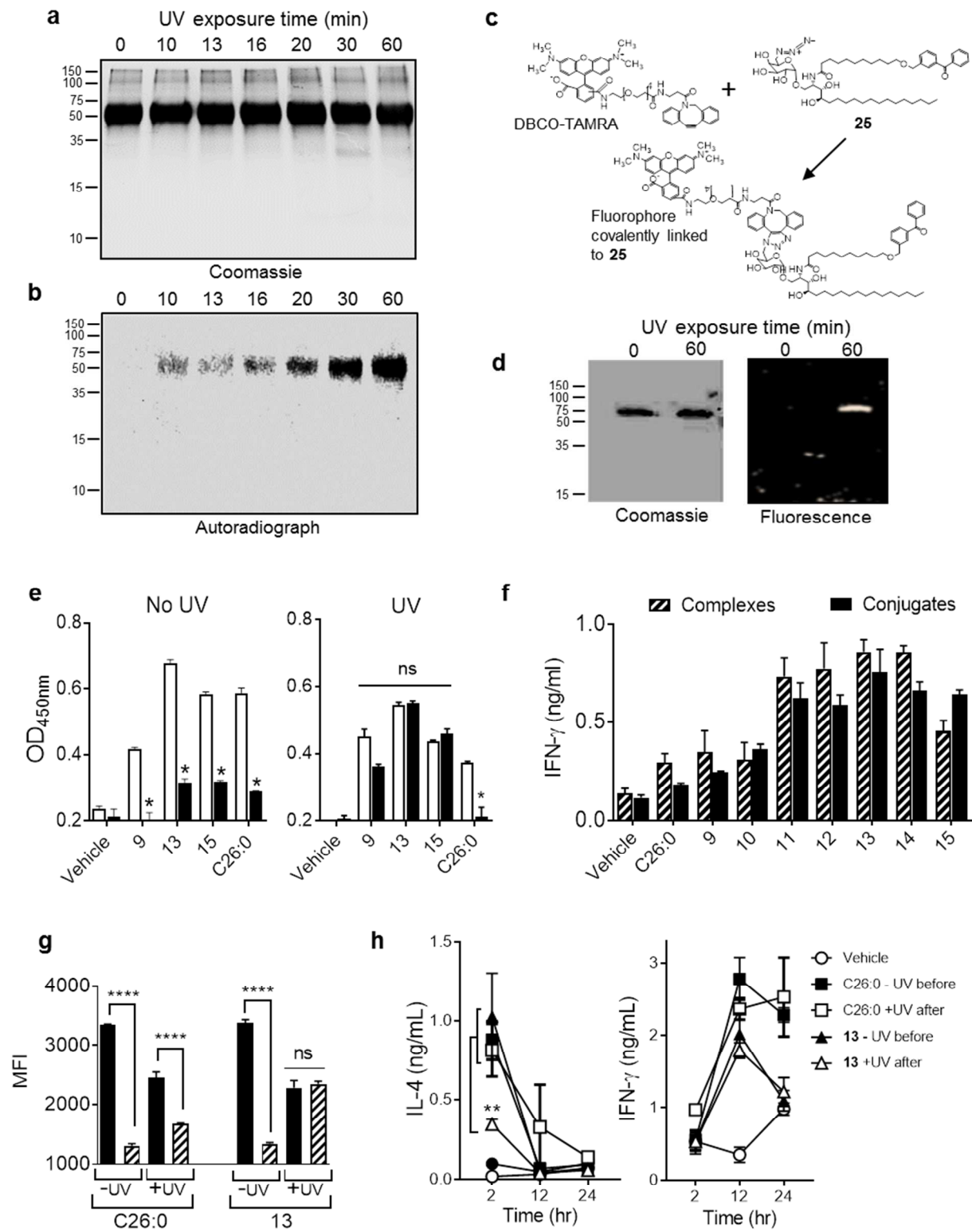
10 7 All symbols and bars are means for triplicate samples, and error bars are  $\pm 1$  SD. \* $P <$   
11 8 0.05, \*\* $P <$  0.01, \*\*\* $P <$  0.001, \*\*\*\* $P <$  0.0001 for comparisons to vehicle treated mice  
12 9 (two-way ANOVA with Dunnett's multiple comparison test). All data are representative  
13 10 of at least three separate experiments.  
14 11  
15 12

### 13 **Formation of covalent CD1d-glycolipid conjugates by photoactivation**

14 14 The known photochemical properties of benzophenones predicted that loading of  
15 15 BPGCs into CD1d proteins followed by exposure to UV irradiation should form  
16 16 covalently stabilized protein-glycolipid conjugates. We validated this initially using a 3-  
17 17 fold molar excess of  $^{14}\text{C}$ -labelled analogue of **13**, compound **26** (Scheme 2, SI) to load  
18 18 soluble recombinant mCD1d protein. Aliquots of the loaded protein were then exposed  
19 19 to a 365 nm UV lamp for times ranging from 0 to 90 minutes, followed by denaturation  
20 20 (1% SDS at 100° C for 5 min) and separation by SDS-PAGE. Staining of the gel with  
21 21 Coomassie blue revealed intact protein in all samples, which ran at the predicted size of  
22 22 ~57 kDa for monomeric soluble CD1d (**Fig. 3a**). Autoradiography of the same gel  
23 23 revealed the presence of the  $^{14}\text{C}$  label co-migrating with CD1d protein in the samples  
24 24 exposed to UV light, but not in the unexposed sample (**Fig. 3b**). Maximum association  
25 25 of radiolabel, indicating the formation of stable protein-glycolipid conjugates that were  
26 26 resistant to denaturation, was achieved following 30 to 60 minutes of UV exposure,

1  
2  
3 1 corresponding to a delivered dose range of 400 – 600 mJoules/cm<sup>2</sup>. Radiometric  
4  
5 2 analysis showed that approximately 70% of CD1d molecules were conjugated to <sup>14</sup>C  
6  
7 3 labeled **26** after 60 minutes of UV exposure (**Supplemental Figure S1**).  
8  
9  
10  
11  
12  
13  
14  
15  
16  
17  
18  
19  
20  
21  
22  
23  
24  
25  
26  
27  
28  
29  
30  
31  
32  
33  
34  
35  
36  
37  
38  
39  
40  
41  
42  
43  
44  
45  
46  
47  
48  
49  
50  
51  
52  
53  
54  
55  
56  
57  
58  
59  
60

1



2

1  
2  
3 **Figure 3: Covalent conjugation of BPGCs to mCD1d.** (a) Coomassie stained gel  
4 and (b) autoradiograph of denaturing SDS-PAGE after exposing mCD1d:  $^{14}\text{C}$ -labelled  
5 analogue of **13**, compound **26** (Scheme 2, SI) complexes (~57 kDa) for various lengths  
6 of time. (c) Diagrammatic representation of click reaction of DBCO-TAMRA dye with  
7 azide-linked-**25** (SI) either loaded non-covalently or covalently conjugated to CD1d  
8 protein. (d) Coomassie stained and fluorescent images of denaturing SDS-PAGE gel of  
9 fluorescently tagged noncovalent-complexes (0 min UV exposure) and covalent-  
10 conjugates (60 min UV exposure) of mCD1d fusion protein (~78 kDa). (e) Complexes  
11 (No UV, left) or conjugates (UV, right) loaded with the indicated BPGC or  $\alpha$ -GC-C26:0  
12 were coated on high binding plates and incubated for 3 days at room temperature either  
13 without (white bars) or with (black bars) washing twice per day with PBS + 0.1% Triton  
14 X-100. Residual glycolipid binding to mCD1d was detected by ELISA using biotinylated  
15 monoclonal antibody L363. \* $P < 0.001$  for multiple t tests of comparisons of washed  
16 versus unwashed samples with each glycolipid. (f) Splenocytes ( $2 \times 10^5$  per well in 0.2  
17 ml complete medium) were stimulated *in vitro* for 18 hours with complexes (hatched  
18 bars) and conjugates (solid bars) immobilized on high binding plates. Supernatants  
19 were collected and assayed for IFN- $\gamma$  by ELISA. (g) JAWS II cells ( $5 \times 10^4$  per well)  
20 pulsed overnight with 100 nM glycolipids (C26:0 or **13**) were either exposed to UV (~400  
21  $\text{mJ}/\text{cm}^2$ ) or left untreated. Cells were stained with L363-AlexaFluor647 either directly  
22 (solid black bars) or after multiple washes (hatched bars) to allow dissociation and  
23 analyzed by flow cytometry. \*\*\*\* $P < 0.0001$ , two-way ANOVA with Bonferroni correction  
24 for indicated comparisons. (h) JAWS II cells were exposed to UV ( $600 \text{ mJ}/\text{cm}^2$ ) either  
25 before (black symbols) or after (white symbols) pulsing with vehicle, C26:0 or **13** at 100  
26 nM concentration. Cells were washed thrice during 24 hours of incubation and  
27 adoptively transferred i.v. into mice ( $3 \times 10^5$  cells per mouse, 4 mice per group). Blood  
28 samples were obtained after 2, 12 and 24 hours to quantitate serum IL-4 and IFN- $\gamma$ . \*\* $P$   
29  $< 0.01$ , two-way ANOVA with Bonferroni correction for indicated comparisons. Data  
30 plotted in (e) – (f) are shown as means for a minimum of three replicates, and error bars  
31 are  $\pm 1$  SD. All experiments were performed at least three times.

1  
2  
3 1 Further analysis of conjugate formation was carried out in studies using  
4  
5 2 compound **25** (synthesis described in SI), an analogue of **13** carrying an azido group at  
6  
7 3 the 6'- position of the saccharide head group (**Fig. 3c**). Complexes formed between this  
8  
9 4 glycolipid and soluble mCD1d were either irradiated with UV  $\lambda$ 365 or not, and then  
10  
11 5 incubated with fluorescent DBCO-TAMRA, which reacts with the azido group of the  
12  
13 6 glycolipid.<sup>17</sup> The samples were then denatured and analyzed by SDS-PAGE. While  
14  
15 7 gels stained with Coomassie blue showed similar CD1d protein in both samples  
16  
17 8 (migrating at ~78 kDa, consistent with the mCD1d fusion protein used for this  
18  
19 9 experiment; see Online Methods for details), only the sample exposed to UV had a  
20  
21 10 fluorescent signal co-migrating with CD1d (**Fig. 3d**). This confirmed the formation of  
22  
23 11 stable conjugates following photoactivation of the benzophenone moiety in CD1d-  
24  
25 12 glycolipid complexes. In addition, the ability of the DBCO-TAMRA reagent to couple to  
26  
27 13 the azido group was consistent with correct orientation of the **13** in the CD1d lipid  
28  
29 14 binding groove, with the carbohydrate head-group exposed and accessible at the  
30  
31 15 surface of the protein.

32  
33  
34  
35  
36  
37 16 To confirm the correct conformation and stability of covalent mCD1d-BPGC  
38  
39 17 conjugates, we tested reactivity with mAb L363, which binds specifically to CD1d loaded  
40  
41 18 with  $\alpha$ -GC in a manner that closely mimics the TCRs of iNKT cells.<sup>18</sup> Plate immobilized  
42  
43 19 mCD1d proteins were loaded with BPGCs, then either UV irradiated or not and tested  
44  
45 20 for binding of L363. This showed binding to levels comparable to that with C26:0  
46  
47 21 loaded mCD1d (**Fig. 3e**). Furthermore, after repeated washing with buffer containing  
48  
49 22 mild detergent to remove reversibly bound glycolipids, we observed significant loss of  
50  
51 23 L363 binding in samples without UV irradiation. In contrast, UV exposed samples  
52  
53  
54  
55  
56  
57  
58  
59  
60



1 loaded with BPGCs showed no significant loss of L363 binding, indicating covalent bond  
2 formation. As expected, L363 binding to mCD1d loaded with C26:0 was reversible  
3 under these conditions with or without UV exposure. To further characterize the  
4 biologic activity of these complexes or conjugates, we also assessed their ability to  
5 stimulate iNKT cell activation in mouse splenocytes (**Fig. 3f**). The UV treated stable  
6 conjugates retained their iNKT cell stimulating activity at levels comparable to  
7 noncovalent complexes, indicating that UV exposure and covalent bond formation did  
8 not adversely alter TCR recognition. Analysis of all seven BPGCs in this assay showed  
9 an influence of the acyl chain spacer length on potency of stimulation, with **13** generally  
10 showing the strongest stimulation.

11 In addition to the analyses of loading and photo-crosslinking to purified  
12 recombinant CD1d proteins, we also assessed the formation of stabilized mCD1d-  
13 glycolipid conjugates on intact CD1d-expressing antigen presenting cells. We used the  
14 murine immortalized dendritic cell line JAWS II for this, since it expresses mCD1d and is  
15 capable of glycolipid antigen presentation.<sup>19</sup> Incubation of these cells with either C26:0  
16 or **13** generated strong surface staining with mAb L363, which for both glycolipids was  
17 greatly reduced following incubation for 1 day in the absence of the glycolipids. In  
18 contrast, exposure of the cells to UV irradiation following culture with the **13** eliminated  
19 any loss of L363 staining with subsequent culture, whereas UV irradiation of C26:0  
20 loaded cells did not prevent decay of L363 binding under the same conditions (**Fig. 3g**).  
21 This strongly suggested that stabilized covalent CD1d-glycolipid conjugates were  
22 produced by UV photoactivation of BPGCs in living cells. This was further evaluated by  
23 testing the ability of JAWS II cells loaded with **13** and UV treated to stimulate iNKT cell

1  
2  
3 1 responses *in vivo* following adoptive transfer of the cells into mice (**Fig. 3h**). We  
4  
5 2 detected strong serum cytokine responses in mice receiving cells bearing the putative  
6  
7 3 covalently stabilized conjugates, and a reduced level of IL-4 relative to IFN- $\gamma$  was  
8  
9 4 observed when compared to injection of cells presenting noncovalent complexes (i.e.,  
10  
11 5 JAWS II cells without UV photoactivation or loaded with C26:0).  
12  
13 6

### 7 **Impact of conjugation on TCR affinity and biologic activity *in vivo***

8 By eliminating dissociation of glycolipid binding to CD1d, we anticipated that conjugation  
9  
10 should increase the overall affinity of cognate interactions with iNKT cell TCRs. To  
11  
12 assess this, fluorescent tetramers of soluble mCD1d loaded with C26:0 or BPGCs were  
13  
14 prepared with and without covalent crosslinking. Binding avidities of tetramers to the  
15  
16 TCRs of mouse iNKT cell hybridoma line DN3A4-1.2 were quantified by measuring  
17  
18 equilibrium binding to the cells over a range of concentrations, as previously  
19  
20 described.<sup>15</sup> Extrapolation of the equilibrium dissociation constant ( $K_D$ ) values showed  
21  
22 maximum avidities for C26:0 and **15** loaded noncovalent complexes, while avidities  
23  
24 declined progressively for BPGCs with shorter acyl tail spacers (**Fig. 4a**). This trend  
25  
26 was not evident with the binding of covalent conjugate tetramers, as the conjugates with  
27  
28 shorter acyl chain variants of BPGCs showed enhanced and more uniform avidities.  
29  
30 These results indicated that dissociation of the glycolipids with shorter acyl tails had a  
31  
32 major impact in TCR avidity, which was reversed by covalent stabilization of the  
33  
34 glycolipid-protein interaction. One apparent exception was the **9** conjugate, which  
35  
36 showed a distinctly lower TCR avidity than the other conjugates tested despite covalent  
37  
38 stabilization.  
39  
40  
41  
42  
43  
44  
45  
46  
47  
48  
49  
50  
51  
52  
53  
54  
55  
56  
57  
58  
59  
60

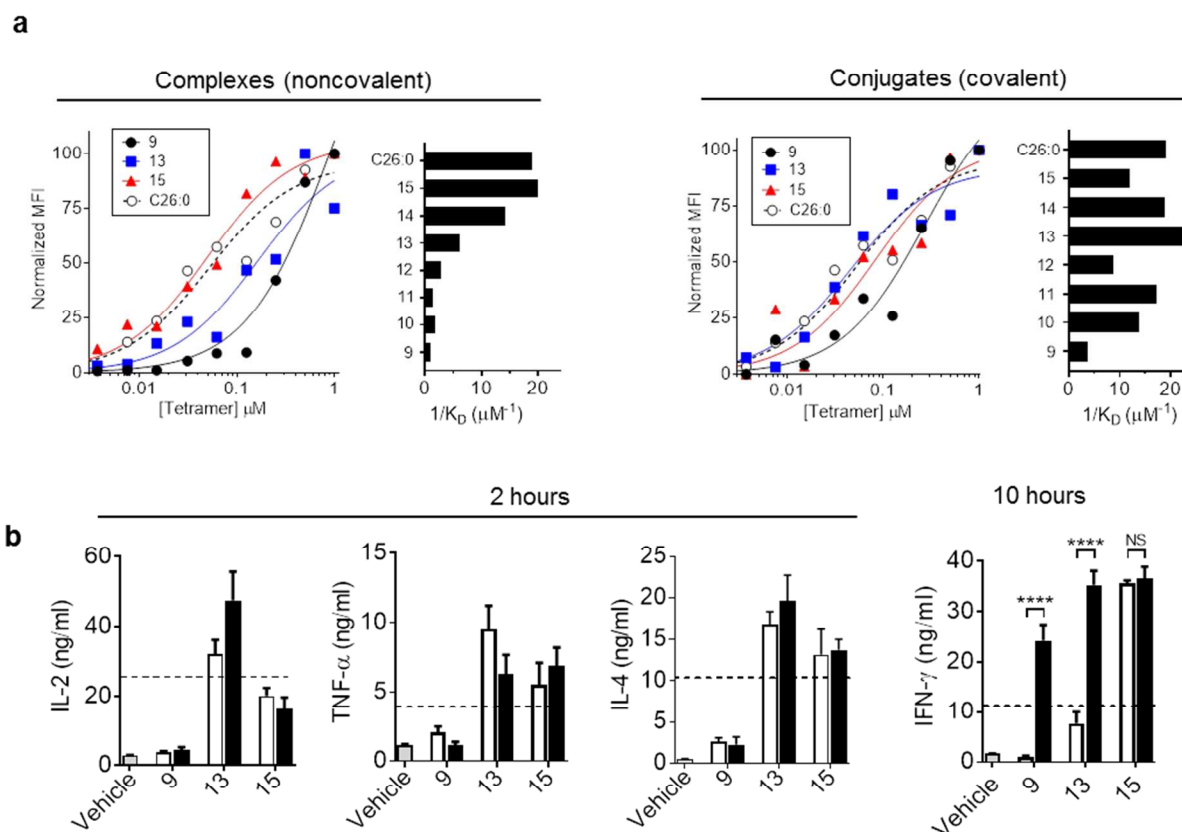


**Figure 4: Affinity for iNKT cell TCR and effects on cytokine profiles. (a)**

Equilibrium binding of mCD1d tetramers loaded with BPGCs over a range of tetramer concentrations was used to assess avidities of complexes (not UV irradiated, left) and conjugates (UV irradiated, right) for TCRs of mouse iNKT cell hybridoma DN3A4-1.2.

Cells stained with tetramers for 1 hour at room temperature were analyzed by flow cytometry. Normalized representative binding curves are shown for three BPGC loaded tetramers, and for standard C26:0 loaded tetramers (not UV irradiated) for comparison (dashed lines). Bar graphs show reciprocal of  $K_D$  values ( $1/EC_{50}$ ) to summarize results for all tetramers.

(b) Serum cytokine levels following i.v. injection of mice with complexes (open bars) or conjugates (filled bars) loaded with the indicated BPGCs. Serum levels are shown at 2 hours post injection for IL-2, TNF- $\alpha$  and IL-4, and at 10 hours for IFN- $\gamma$ . Background levels of cytokines in sera from mice injected with inert aqueous vehicle (gray bars), and levels for mice injected with 4 nmoles of free C26:0 glycolipid (horizontal dashed lines) are shown for reference. Bars represent means for groups of 4 animals each, and error bars show 1 SD. \*\*\*\* $P < 0.0001$  for conjugate

1  
2  
3 1 versus complex in the indicated comparisons (2-way ANOVA with Bonferroni's multiple  
4 2 comparisons test). NS, not significant ( $P > 0.05$ ). Differences were not significant for  
5 3 other comparisons shown between complexes and conjugates.  
6  
7  
8  
9 4

10 5 We next assessed the *in vivo* activities of soluble mCD1d-BPGC complexes and  
11 6 conjugates using three different BPGCs that varied in their affinities for iNKT cell TCRs.  
12 7 After a single i.v. injection of mCD1d complexes or conjugates loaded with **9**, **13** or **15**  
13 8 (30  $\mu\text{g}$  of mCD1d protein containing  $\sim 0.4$  nmoles of each glycolipid), serum levels of IL-  
14 9 2, TNF- $\alpha$ , IL-4 and IFN- $\gamma$  were determined at 2, 10 and 24 hours after administration  
15 10 (**Fig. 4b, and Supplemental Fig. S2**). Injection of C26:0 as a free glycolipid was used  
16 11 as a standard which is known to activate iNKT cell-dependent release of various  
17 12 cytokines, such as IL-2, TNF- $\alpha$  and IL-4 which peak in serum at approximately 2 hours,  
18 13 and IFN- $\gamma$  which peaks at 10-12 hours after the injection.<sup>20</sup> The administration of  
19 14 conjugates formed with **13** or **15** activated secretion of all four cytokines, including  
20 15 levels of IL-2, TNF- $\alpha$  and IL-4 at 2 hours and IFN- $\gamma$  at 10 hours, that equaled or  
21 16 exceeded those stimulated by free C26:0. Noncovalent complexes gave similar  
22 17 stimulation as conjugates at 2 hours, but the level of IFN- $\gamma$  at 10 hours was significantly  
23 18 higher with conjugates for **13**, and also for conjugates with **9** which did not stimulate any  
24 19 detectable serum cytokines at 2 hours. These findings confirmed the iNKT cell  
25 20 activating properties of soluble complexes and conjugates *in vivo*, and also were  
26 21 consistent with the ability of covalent conjugation to stabilize the shorter **9** and **13**  
27 22 glycolipids, extending the duration of their bioactivity. In addition, covalently stabilized **9**  
28 23 conjugates showed a remarkable skewing of the cytokine response such that only IFN- $\gamma$   
29 24 was detected among the cytokines measured.  
30  
31  
32  
33  
34  
35  
36  
37  
38  
39  
40  
41  
42  
43  
44  
45  
46  
47  
48  
49  
50  
51  
52  
53  
54  
55  
56  
57  
58  
59  
60

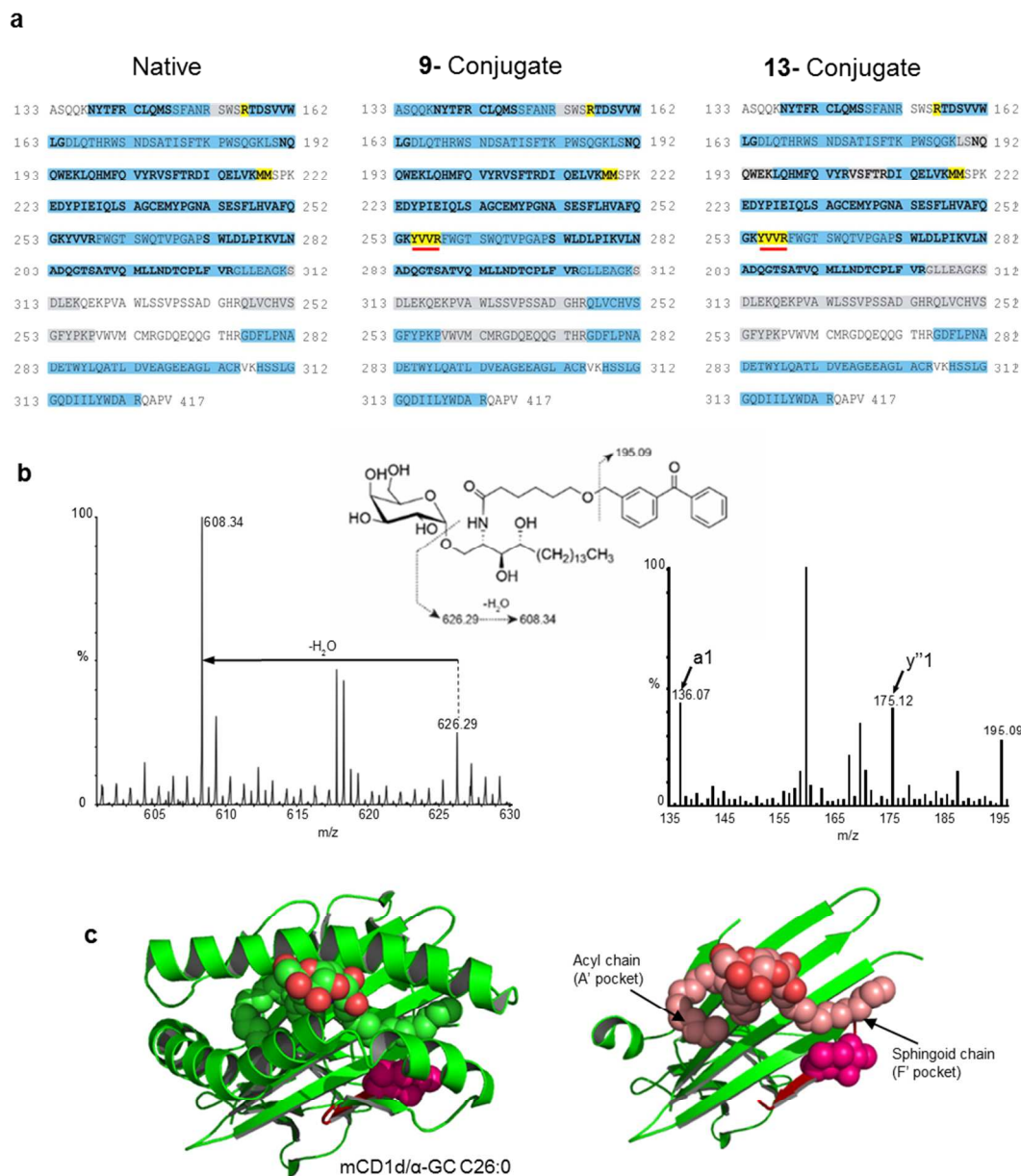


**Figure 5: Mapping of covalent attachment site.** (a) Peptide mapping summaries from nano-LC-ES-MS<sup>E</sup> analyses are shown for unloaded mCD1d fusion protein (native) and for protein-glycolipid conjugates containing either **9** or **13**, focusing on the lipid binding region comprising the  $\alpha$ 1 and  $\alpha$ 2 regions of CD1d. Amino acid sequences of mCD1d  $\alpha$ 1 through  $\alpha$ 2 domains are shown in single letter code. Bold text indicates residues forming the lipid binding pocket, blue shading indicates residues mapped with a high degree of confidence, and grey shading indicates residues mapped with a good degree of confidence. Residues highlighted in yellow indicate amino acids that were not

1  
2  
3 1 observed in any detected peptides. Peptides containing the four amino acids  
4 underlined in red in both conjugates were detected with high confidence in the native  
5 protein but, were absent in both conjugates. (b) MS<sup>E</sup> analysis of the doubly charged ion  
6 m/z 661.33 observed at 30.9 min elution time in the analysis of a reduced,  
7 carbamidomethylated, PNGase-F treated tryptic digest of the **9** conjugate. The  
8 molecular ion is consistent with the tryptic peptide containing the <sup>255</sup>YVVR<sub>258</sub> residues  
9 modified by a single C6 glycolipid moiety. Labelled ions in the left panel show loss of  
10 water from a cleaved C6 BPGC entity, while the right panel highlights evidence for the  
11 peptide with the y''1 ion for the C-terminal arginine at m/z 175 and the a1-ion for the N-  
12 terminal tyrosine at m/z 136. The ion at m/z 195 is consistent with loss of the  
13 benzophenyl group from the BPGC molecule. (c) The mCD1d protein structure  
14 previously deduced from X-ray crystallography (PDB number 3HE6) is shown as a  
15 ribbon diagram in green, and the two valine residues comprising the proposed covalent  
16 attachment site are shown as bright pink spheres. The view on the left shows the intact  
17  $\alpha$ 1 and  $\alpha$ 2 domains with  $\alpha$ -GC C26:0 (green and red spheres) bound in the lipid binding  
18 groove. In the view on the right, the  $\alpha$ -helices forming the roof of the groove have been  
19 removed, and the bound glycolipid is shown as pink and red spheres.

### 19 **Analysis of conjugation site by peptide mapping**

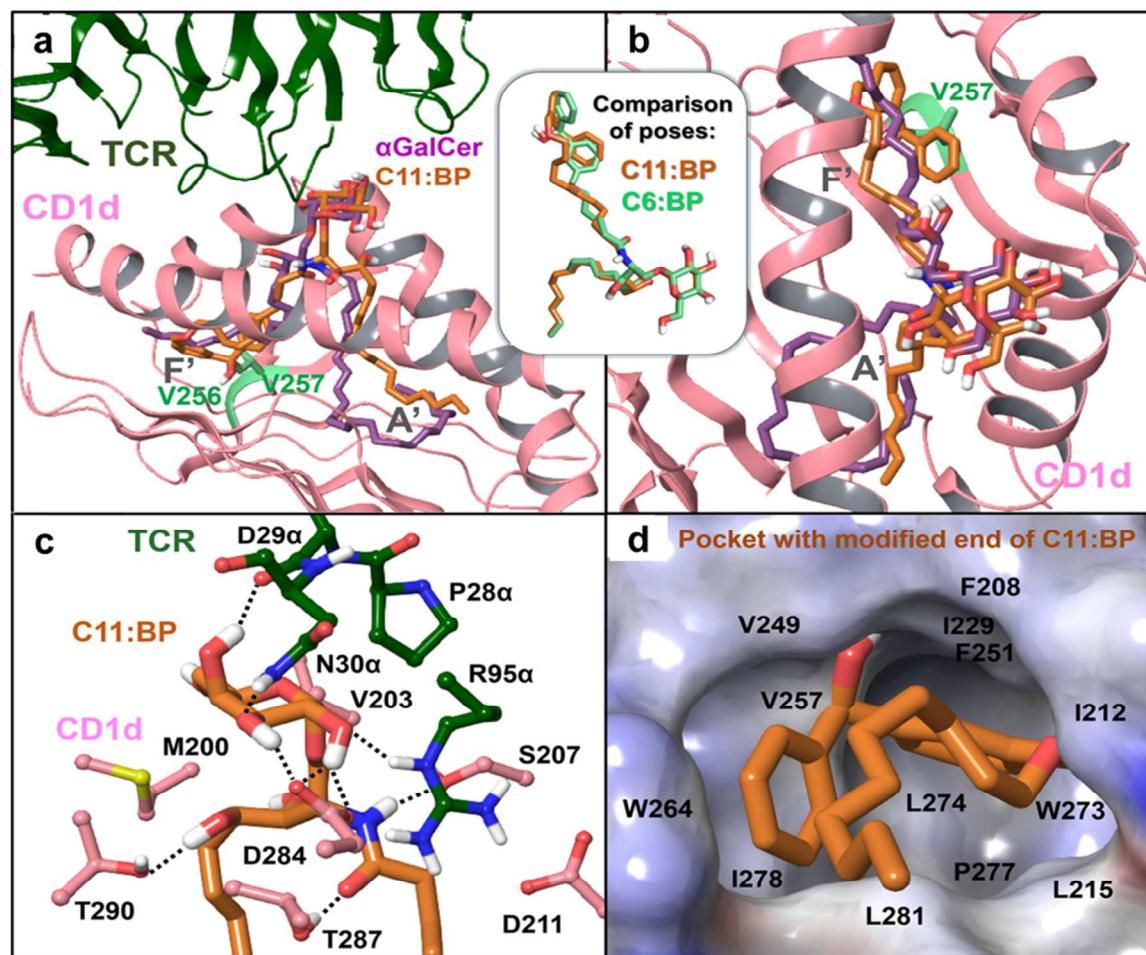
20 Peptide mapping analyses of samples of native mCD1d and mCD1d conjugates with **9**  
21 and **13** were performed to identify possible sites of conjugation. Samples with or without  
22 enzymatic deglycosylation were digested with trypsin, or with trypsin plus chymotrypsin.  
23 Digested samples were analysed by online nano-liquid chromatography-electrospray  
24 tandem mass spectrometry (nano-LC-ES-MS<sup>E</sup>) (**Supplemental Fig.S4**). For native  
25 mCD1d samples, peptides covering the entirety of the glycolipid binding domains were  
26 consistently mapped with a high degree of confidence for all but three residues (R156,  
27 M218 and M219) of the putative binding site. Both the **9** and **13** conjugated samples  
28 produced very similar data to that of the native mCD1d, with the notable exception that

ions covering the unmodified region  ${}_{255}\text{YVVR}_{258}$  were not observed (**Fig. 5a**, and **Supplemental Tables S1 – S3**). Instead, molecular ions consistent with the presence of a **13** or **9** modification were detected (**Supplemental Figures S4 and S5**), and fragmentation of these modified peptides produced signals corresponding to both the *N*-terminal tyrosine and the C-terminal arginine, as well as *y*'- and *b*-ions consistent with modified VVR and YVV (**Fig. 5b**). Although definitive evidence for covalent modification of a specific residue was not obtained, these data strongly supported the site of conjugation to be in the region  ${}_{255}\text{YVVR}_{258}$ , with one or both valine residues at the base of the F' pocket of mCD1d being directly involved in the formation of potential bioconjugation products (**Fig. 5C and Supplemental Fig. S6**).

### 12 **Modelling BPGC analogue binding modes.**

To confirm the feasibility of the putative conjugation site identified in mCD1d, the binding modes of **9** and **13** were modelled into the published crystal structure of the ternary complex of CD1d with  $\alpha$ -GC C26:0 and the  $V\alpha 14$ - $V\beta 8.2$  iNKT cell TCR (PDB entry code 3HE6) (**Fig. 5c and Fig. 6**). Briefly, compound **13** was docked without its benzophenone group, which was deleted prior to docking. The binding of the modified benzophenone group (i.e., diphenylmethanol, formed by the benzophenone group after conjugation) was predicted in a separate docking run considering that the flexible linker in the BPGC analogues would only minimally restrain possible binding conformations of the end group. The most favorable docking pose showed excellent shape complementarity and non-polar contacts in the binding site while linked covalently to the V257 side chain in the F' pocket. The diphenylmethanol pose and the sugar moiety of

1 **13** docked without the benzophenone end group were then connected by predicting an  
 2 optimal conformation for the flexible linker between them through docking the linker  
 3 segment (with constraints). Models of the full **9** and **13** structures were generated  
 4 through splicing in the appropriate linkers of the two BPGC analogues, and were then  
 5 refined using Prime complex structure refinement in Schrödinger software (**Fig. 6**).



6  
 7 **Figure 6: Molecular docking of 13 and 9 in mCD1d.** (a, b) Two views of the  
 8 binding model of **13** and co-crystallized  $\alpha$ -GC (from PDB code 3HE6). The inset  
 9 compares the binding models of **13** (C11:BP) and **9** (C6:BP). The modified end in the  
 10 F' pocket is covalently attached to V257 (residue V125 in the structure with PDB code  
 11 3HE6). (c) Interactions near the sugar moiety of **13**. A TCR interaction shared between  
 12  $\alpha$ -GC C26:0 in the crystal structure and both **9** and **13** models was the hydrogen-



1 bonding interaction of the galactose 3''-OH with N30 $\alpha$ . Additional stabilizing interactions  
2 with the sugar moiety of the bound BPGCs included hydrogen bonds with TCR residues  
3 R95 $\alpha$  and D29 $\alpha$  and with D284 of mCD1d. The binding site that in the crystal structure  
4 is occupied by the vicinal diol of the phytosphingosine chain of  $\alpha$ -GC was occupied in  
5 the BPGC bound models by a less bulky amide group. This allowed reorientation of the  
6 TCR $\alpha$  R95 side chain (R95 $\alpha$ ) into the same region, forming a favourable stacking  
7 interaction between the guanidinium of the arginine and the amide of the ligand. The  
8 guanidinium of R95 $\alpha$  was also sandwiched between the mCD1d residues D284 and  
9 D211, salt-bridging with both aspartates. Other interactions stabilizing the predicted  
10 BPGC binding orientation were apparent, such as hydrogen bonds between the amide  
11 group and residues S207 and T287 of mCD1d, and between the C3 hydroxyl of the  
12 phytosphingosine chain and residue T290 of mCD1d. **(d)** CD1d surface in the region of  
13 the modified terminal, colored by electrostatic potential (blue indicates nonpolar and red  
14 indicates polar surfaces). The end group forms favourable non-polar contacts with I229,  
15 V249, F251, W264, W273, L274, I278 and L281 (residue numbers are based on the  
16 mCD1d-fusion protein).

17  
18 The final refined structures of **9** and **13** glycolipids after docking showed similar  
19 binding modes except for the linker region, as expected (**Fig. 6, inset**). Compared to  
20 the corresponding sugar moiety of  $\alpha$ -GC C26:0 in the crystal structure, the  
21  $\alpha$ -galactopyranosyl group in BPGC analogues was positioned closer to the TCR and  
22 slightly shifted (**Fig. 6a**). The lipid chains occupying the A' and F' pockets in the models  
23 with bound BPGCs were switched compared to the orientation of  $\alpha$ -GC C26:0 in the  
24 crystal structure. Thus, the acyl chain of the covalently bound **9** and **13** was positioned  
25 in the F' pocket of mCD1d, rather than in the A' pocket as in the case of the  
26 noncovalently bound  $\alpha$ -GC C26:0 (**Fig. 6a and b**). This binding orientation allowed  
27 reorientation of the TCR $\alpha$  R95 side chain (R95 $\alpha$ ) to form a favourable stacking

1  
2  
3 1 interaction between the guanidinium of the arginine and the amide of the ligand, as well  
4  
5 2 as a number of other stabilizing interactions (**Fig. 6c**). The acyl chains of **9** and **13**  
6  
7 3 adopted quite similar orientations in the two BPGC models in spite of their different  
8  
9 4 lengths, linking the diphenylmethanol moiety covalently bound to the side chain of V257  
10  
11 5 in a mainly non-polar pocket (**Fig. 6d**).  
12  
13  
14  
15  
16

## 17 **Discussion**

18  
19 8 In this study we synthesized a series of benzophenone-modified glycolipids that can be  
20  
21 9 covalently cross-linked to soluble as well as surface expressed CD1d to generate highly  
22  
23 10 stable conjugates that activate iNKT cells *in vitro* and *in vivo*. By appending a  
24  
25 11 photoactivatable benzophenone group to the end of the amide linked acyl chain of  
26  
27 12  $\alpha$ -GC, we generated a family of BPGCs with varying aliphatic spacer lengths.  
28  
29  
30 13 Screening for biologic activity using a variety of assays for iNKT cell stimulation showed  
31  
32 14 that all of these BPGCs could be presented by CD1d, with most experiments showing  
33  
34 15 **13** to be optimal for iNKT cell stimulation. Using relatively brief and low energy UV  
35  
36 16 irradiation, all of the BPGCs could be activated to form stable conjugates with purified  
37  
38 17 CD1d proteins. In addition, UV photoactivation could be shown to stabilize BPGC  
39  
40 18 interactions with CD1d expressed in living cells. By multiple criteria, UV induced  
41  
42 19 covalent conjugates of BPGCs retained their interactions with iNKT cell TCRs, and  
43  
44 20 conjugates in either soluble, surface bound or cell associated forms possessed the  
45  
46 21 ability to activate cytokine secretion by iNKT cells.  
47  
48  
49  
50

51 22 Our primary goal in developing BPGCs was to use conjugate formation with  
52  
53 23 CD1d as a method for improving delivery of iNKT cell activators as potential agents for  
54  
55 24 immunotherapy. Particularly in the case of cancer immunotherapy, many studies in  
56  
57  
58  
59  
60

1 mouse models have highlighted the potential for iNKT cell activators to deliver striking  
2 anti-cancer effects.<sup>4c</sup> However, administration of  $\alpha$ -GC as a free glycolipid has the  
3 potential for dose limiting toxicity, and also leads to the rapid development of a long-  
4 lived hyporesponsive state (anergy) that interferes with repeated treatments.<sup>10, 21</sup> Most  
5 likely, these issues contribute to the limited efficacy of free  $\alpha$ -GC injections observed so  
6 far in early phase clinical trials for cancer in humans.<sup>9, 22</sup> Approaches to more precisely  
7 deliver  $\alpha$ -GC to overcome these problems have been developed, including the  
8 administration of *ex vivo* glycolipid loaded antigen presenting cells or targeted soluble  
9 recombinant CD1d proteins.<sup>4c, 8a, 8c, 8d</sup> These approaches have shown improved  
10 outcomes in animal models, as well as in limited clinical studies in cancer patients<sup>4c, 6b,</sup>  
11 <sup>23</sup>. However, the ability of  $\alpha$ -GC to dissociate from these delivery vehicles after *in vivo*  
12 injection remains a suboptimal feature. The use of BPGCs to covalently lock the  
13 glycolipid onto CD1d in an active configuration, as shown in the current study,  
14 represents a method for improving these delivery methods, and achieving more focused  
15 and effective immunotherapy without the limitations or toxic effects of systemic  $\alpha$ -GC  
16 injections.

17 Detailed analysis of the effects of variation in the length of the acyl chain spacer  
18 in the BPGCs revealed some interesting and potentially important findings. First, we  
19 noted that the **9** and **10** compounds had very low TCR affinity and low stimulatory  
20 activity when not covalently linked to CD1d (**Figs. 3f and 4a**), presumably because of  
21 their rapid dissociation. However, with conjugate formation these glycolipids showed  
22 improved affinity and enhanced iNKT cell stimulation. This suggests that the BPGCs  
23 with shorter acyl chains, even if released by some mechanism after conjugation, should

1  
2  
3 1 be less likely to induce unwanted effects such as iNKT cell anergy or systemic toxicity.  
4  
5 2 Another notable finding was that **9**, which even after conjugation continued to show a  
6  
7 3 lower TCR affinity than the other BPGCs, also gave a remarkably biased cytokine  
8  
9 4 response (i.e., significant IFN- $\gamma$  levels with no detectable IL-4 or other cytokines) when  
10  
11 5 injected in the form of a conjugate with soluble CD1d protein (**Fig. 4b**). This type of  
12  
13 6 “Th1-biased” cytokine response has been repeatedly associated in previous studies  
14  
15 7 with analogues of  $\alpha$ -GC that provide superior anti-tumor responses in mouse models.<sup>24</sup>  
16  
17 8 Thus, through alterations in the length of the acyl chain spacer, it should be possible to  
18  
19 9 tune the responses to BPGC conjugates in terms of affinity and biologic response to  
20  
21 10 optimize desired therapeutic outcomes.  
22  
23  
24  
25

26 11 Our mapping of the site of covalent bond formation in **9** and **13** conjugates  
27  
28 12 yielded the surprising finding of a single major conjugation site for both glycolipids.  
29  
30 13 Another surprising aspect of this result was that the specific region of CD1d that was  
31  
32 14 implicated was located near the base of the F' pocket, which in all CD1d-glycolipid  
33  
34 15 complexes resolved by X-ray crystallography would be predicted to be in greater  
35  
36 16 proximity to the sphingoid base than the acyl tail of the glycolipid (**Fig. 5c**).<sup>2</sup> However,  
37  
38 17 this apparent switch in the orientation of the two lipid tails of the glycolipid can be readily  
39  
40 18 accommodated in energetically favorable poses of the glycolipid in molecular models  
41  
42 19 (**Fig. 6**). Thus, our findings suggest the possibility of greater flexibility in the lipid  
43  
44 20 binding process of CD1d, which has only been occasionally hinted at in atomic level  
45  
46 21 structure studies.<sup>25</sup> Further structural analyses of CD1d-BPGC conjugates should  
47  
48 22 enable new types of analyses to expand our understanding of the unique process of  
49  
50  
51  
52  
53  
54  
55  
56  
57  
58  
59  
60

1 glycolipid antigen presentation, as well as opportunities for improving immunotherapies  
2 that target iNKT cells.

## 3 4 **EXPERIMENTAL METHODS**

5  
6 **Synthesis and compound characterization.** Full experimental details of the synthesis  
7 and characterization of all compounds used in this study are provided in the  
8 **Supplementary Information.**

9  
10 **Mice.** Female C57BL/6J (B6) mice 6–8 weeks old were obtained from Jackson  
11 Laboratories or Taconic and maintained in pathogen-free conditions. All experiments  
12 requiring mice were conducted in compliance with institutional guidelines and under an  
13 authorization delivered by the Institute of Animal Use and Biosafety Committee at Albert  
14 Einstein College of Medicine.

15  
16 **Cell lines, clones and hybridomas.** HeLa cells transfected with human CD1d  
17 (HeLa.hCD1d) were cultured in DMEM supplemented with 10% FBS, and JAWS II cells  
18 were cultured in  $\alpha$ -MEM supplemented with 10% FBS and 20 ng/ml murine GM-CSF.  
19 Mouse splenocytes were maintained in RPMI with 10% FBS. BMDCs were prepared as  
20 described earlier and cultured in RPMI supplemented with 10% FBS. Mouse iNKT  
21 hybridoma DN3A4-1.2 was maintained in complete RPMI medium containing 10%  
22 de complemented serum.<sup>26</sup> Human iNKT clonal HDE3 was clonally expanded by  
23 stimulation with PHA-P in the presence of recombinant human IL-2 at 250 IU/ mL ,  
24 recombinant human IL-7 at 10 ng/mL and allogeneic PBMCs (irradiated at 5000 rad),

1  
2  
3 1 and cultures were fed by addition of fresh medium containing IL-7 and IL-2 every 2-3  
4  
5 2 days.<sup>8d, 15</sup>  
6  
7  
8  
9

10 4 **Recombinant CD1d proteins and monoclonal antibody L363.** Single chain  $\beta$ 2m-  
11  
12 5 mouse CD1d-hexahistidine (MW ~57 kDa) and human CD1d- $\beta$ 2m-hexahistidine were  
13  
14 6 purified from CHO cells stably transfected with respective genes.<sup>27 15</sup> Single chain  
15  
16 7 mCD1d- $\beta$ 2m with a C-terminal single chain immunoglobulin Fv fusion (mCD1d- $\beta$ 2m-  
17  
18 8 ScFv, MW ~78 kDa) was produced in transiently transfected HEK cells and purified as  
19  
20 9 previously described.<sup>8c, 8d</sup> The ScFv moieties of these proteins were specific for the  
21  
22 10 human tumor associated antigens CEA or C35, although their specific binding  
23  
24 11 properties were not relevant to experiments in the current study.  
25  
26  
27

28 12 To determine the affinity of mCD1d-BPGC tetramers for iNKT-cell TCRs,  $1 \times 10^4$   
29  
30 13 DN3A4-1.2 cells were stained with a range of concentrations of tetramers loaded with  
31  
32 14 the different glycolipids to form complexes. Soluble mCD1d proteins were prepared and  
33  
34 15 biotinylated following published methods with minor modifications.<sup>28</sup> Glycolipids were  
35  
36 16 prepared and loaded onto soluble mCD1d as described in the following section. In  
37  
38 17 some cases, the loaded mCD1d complexes were converted to covalent conjugates by  
39  
40 18 exposure to UV irradiation for 60 minutes in solution (400 mJoules/cm<sup>2</sup>). Formation of  
41  
42 19 tetramers, equilibrium binding of tetramers to NKT cells, and measurement of binding by  
43  
44 20 flow cytometry has been previously described in detail.<sup>15</sup>  
45  
46  
47  
48

49 21 Monoclonal antibody L363, specific for mCD1d with bound  $\alpha$ -GC C26:0 and other  
50  
51 22 related forms of  $\alpha$ -GC, has been previously described<sup>15, 18, 29</sup> The antibody was purified  
52  
53 23 from supernatants of the cultured hybridoma line, and was biotinylated using sulfo-NHS  
54  
55  
56  
57  
58  
59  
60

1 biotinylation kit or fluorescently tagged with Alexa Fluor 647 (Alexa 647 labelling kit,  
2 Thermo Fisher). Binding of fluorescently labeled L363 to cells was determined by flow  
3 cytometry using an LSR II cytometer (BD Biosciences) and FlowJo software.<sup>15, 19</sup>

4  
5 **CD1d loading and covalent crosslinking.** Glycolipids dissolved in DMSO at 1 mg/ml  
6 were diluted to 100  $\mu$ M concentration in appropriate volumes of PBS and PBS plus  
7 0.1% Triton X-100 to yield final DMSO concentration of 8-10% and 0.05% Triton X-100.  
8 Glycolipids were added to CD1d at a molar ratio of 3:1 in PBS plus 0.05% Triton X-100  
9 (for *in vitro* applications) or PBS + 0.05% Tween-20 (for *in vivo* applications), and  
10 incubated for 12-18 hours for complete loading of the complexes. Loaded complexes  
11 were transferred to ultra-low binding microtiter plate wells and cooled on ice. A fixed  
12 wavelength UV lamp (Schleicher & Schuell, RAD-FREE long wave UV lamp,  $\lambda = 365$   
13 nm) was placed directly over wells containing complexes for 1 hour on ice. Resulting  
14 conjugates were recovered from the wells and excess glycolipid and detergent was  
15 removed using detergent-removal columns (Pierce).

16 An azide-functionalized **13** was employed to determine the efficiency of covalent  
17 cross-linking. The azido-**13** conjugates and complexes were covalently coupled to  
18 dibenzenecyclooctyne tetramethylrhodamine (DBCO-TAMRA, Click Chemistry Tools)  
19 by Huisgen cycloaddition.<sup>17</sup> The ternary complex thus obtained was denatured using  
20 DTT and SDS and run on SDS-PAGE for detection. To determine stability of  
21 conjugates, the complexes and conjugates were coated onto high binding 96 well plates  
22 and washed with PBS-Tx 0.05% every 12 hours for three days to remove reversibly  
23 bound glycolipids. Plates were incubated at room temperature between washes.

1 For detection of mCD1d-glycolipid complexes and conjugates on glycolipid  
2 pulsed JAWS II cells, the cells were plated at  $5 \times 10^4$  cells per well in microtiter plates  
3 and cultured with 100 nM of either  $\alpha$ -GC C26:0 or **13** for 18 hours, followed by one wash  
4 with medium and then UV irradiation if indicated for 30 minutes (~400  
5 mJ/cm<sup>2</sup>). Samples of UV exposed and non-exposed cells were stained with mAb L363  
6 coupled with AlexaFluor 647 and analyzed by flow cytometry using an LSR II flow  
7 cytometer (BD Biosciences) to determine surface bound glycolipid-CD1d complexes or  
8 conjugates (solid black bars), before and after incubation for two days to allow  
9 dissociation of glycolipids.

10  
11 ***In vitro* and *in vivo* iNKT-cell stimulation assays.** To determine the EC<sub>50</sub> of BPGCs,  
12 BMDCs from C57BL/6 mice or human CD1d transfected HeLa cells (HeLa.hCD1d) were  
13 cultured in microtiter plate wells ( $5 \times 10^4$  BMDC and  $1 \times 10^4$  HeLa.hCD1d per well), and  
14 pulsed with varying BPGC concentrations ranging between 50  $\mu$ M and 0.01 nM in 100  
15  $\mu$ l of culture medium per well for 3 hours at 37 °C. Cells were washed once to remove  
16 unbound glycolipid. The iNKT hybridoma DN3A4-1.2 or human iNKT clone HDE3 were  
17 then added ( $5 \times 10^4$  cells per well in 0.2 ml medium), and the cultures were maintained  
18 for 12 – 18 hours at 37°C. Stimulation was determined by measuring supernatant levels  
19 of IL-2 for DN3A4 1.2 or IFN- $\gamma$  for HDE3 by capture ELISA as described.<sup>30</sup> Cytokine  
20 response was plotted against dose and EC<sub>50</sub> was calculated using the function log  
21 agonist against response in Prism software.

22 To determine the serum cytokine levels induced *in vivo* in mice by administration  
23 of free glycolipids, glycolipid-loaded mCD1d complexes and conjugates, or *ex vivo*



1 glycolipid loaded JAWS II cells, mice were bled at 2, 10 and 24 hours following i.v.  
2 injections and serum samples were prepared. For free glycolipids, mice (3-5 per group)  
3 received 4 nanomoles of  $\alpha$ -GC C26:0, **9**, **13** or **15**. For comparison of *in vivo* activity of  
4 conjugates, complexes and free glycolipids, 30  $\mu$ g/mouse of complexes or conjugates or  
5 equimolar amounts of free BPGCs (0.4 nanomoles) were injected into mice i.v. Serum  
6 cytokine levels were measured by capture ELISA.

7  
8 **Mass spectrometry and proteomic analyses.** Tryptic and chymotryptic peptide digest  
9 mixtures of native mCD1d or conjugates were analysed either directly by on-line nano-  
10 liquid chromatography (nano-LC) electrospray (ES) MS and MS/MS, or subjected to *N*-  
11 linked glycan release by PNGase F followed by subdigestion with additional proteases  
12 prior to analysis. For detailed method see Supplemental Methods section.

13  
14 **Computational molecular modeling and docking studies.** Binding modes of **9** and  
15 **13** glycolipids to mCD1d were predicted using the mCD1d/ $\alpha$ -GC/TCR crystal structure  
16 with PDB entry code 3HE6, containing V $\alpha$ 14-V $\beta$ 8.2 iNKT TCR (mouse variable, human  
17 constant domains). The crystal structure was prepared using Protein Preparation  
18 Wizard tools (Schrödinger software package, version 2016-1). For detailed method see  
19 Supplemental Methods section.

20  
21 **Statistical analysis.** Results are expressed as mean  $\pm$  SEM. Statistical significance  
22 between the groups was determined with multiple t tests, one-way-ANOVA or two-way-

1  
2  
3 1 ANOVA tests with the Bonferroni correction as indicated. All statistical analyses were  
4  
5 2 done using GraphPad Prism software.  
6  
7  
8 3  
9

#### 10 4 **Acknowledgments**

11  
12 5 Major funding support was provided by NIH/NIAID grant R01 AI45889 and U01  
13  
14 6 GM111849 (to SAP). GSB acknowledges support in the form of a Personal Research  
15  
16  
17 7 Chair from Mr. James Bardrick and a Royal Society Wolfson Research Merit Award.  
18  
19 8 SMH and SJN were supported by Biotechnology and Biological Sciences Research  
20  
21 9 Council Grant BB/K016164/1. Flow cytometry and recombinant protein production were  
22  
23 10 supported by core facilities of the Albert Einstein College of Medicine Cancer Center  
24  
25 11 (NCI grant CA13330). We thank Drs. Alena Donda (Ludwig Cancer Institute) and Amy  
26  
27 12 Howell (University of Connecticut) for helpful discussions.  
28  
29  
30  
31 13

#### 32 14 **Competing financial interests**

33  
34  
35 15 MZ is an employee of Vaccinex, Inc., which has proprietary interests in iNKT cell-based  
36  
37 16 immunotherapeutics. SAP is a paid consultant of Vaccinex, Inc. The other authors  
38  
39 17 declare no competing financial interests.  
40  
41  
42 18  
43  
44

#### 45 19 **Additional information**

46  
47 20 Any supplementary information, chemical compound information and source data are  
48  
49 21 available in the online version of the paper.  
50  
51  
52 22  
53

#### 54 23 **References**

55  
56 24  
57  
58  
59  
60

1. Brennan, P. J.; Brigl, M.; Brenner, M. B., Invariant natural killer T cells: an innate activation scheme linked to diverse effector functions. *Nature reviews. Immunology* **2013**, *13* (2), 101-17.
2. Rossjohn, J.; Pellicci, D. G.; Patel, O.; Gapin, L.; Godfrey, D. I., Recognition of CD1d-restricted antigens by natural killer T cells. *Nature reviews. Immunology* **2012**, *12* (12), 845-57.
3. Laurent, X.; Bertin, B.; Renault, N.; Farce, A.; Specca, S.; Milhomme, O.; Millet, R.; Desreumaux, P.; Henon, E.; Chavatte, P., Switching invariant natural killer T (iNKT) cell response from anticancerous to anti-inflammatory effect: molecular bases. *J Med Chem* **2014**, *57* (13), 5489-508.
4. (a) Kawano, T.; Cui, J.; Koezuka, Y.; Toura, I.; Kaneko, Y.; Motoki, K.; Ueno, H.; Nakagawa, R.; Sato, H.; Kondo, E., et al., CD1d-restricted and TCR-mediated activation of valpha14 NKT cells by glycosylceramides. *Science* **1997**, *278* (5343), 1626-9; (b) Motoki, K.; Morita, M.; Kobayashi, E.; Uchida, T.; Akimoto, K.; Fukushima, H.; Koezuka, Y., Immunostimulatory and antitumor activities of monoglycosylceramides having various sugar moieties. *Biological & pharmaceutical bulletin* **1995**, *18* (11), 1487-91; (c) Nair, S.; Dhodapkar, M. V., Natural Killer T Cells in Cancer Immunotherapy. *Front Immunol* **2017**, *8*, 1178.
5. (a) Cerundolo, V.; Salio, M., Harnessing NKT cells for therapeutic applications. *Curr Top Microbiol Immunol* **2007**, *314*, 325-40; (b) Cerundolo, V.; Silk, J. D.; Masri, S. H.; Salio, M., Harnessing invariant NKT cells in vaccination strategies. *Nature reviews. Immunology* **2009**, *9* (1), 28-38.
6. (a) Kharkwal, S. S.; Arora, P.; Porcelli, S. A., Glycolipid activators of invariant NKT cells as vaccine adjuvants. *Immunogenetics* **2016**, *68* (8), 597-610; (b) Exley, M. A.; Nakayama, T., NKT-cell-based immunotherapies in clinical trials. *Clin Immunol* **2011**, *140* (2), 117-8.
7. (a) Birkholz, A. M.; Kronenberg, M., Antigen specificity of invariant natural killer T-cells. *Biomed J* **2015**, *38* (6), 470-83; (b) Carreno, L. J.; Saavedra-Avila, N. A.; Porcelli, S. A., Synthetic glycolipid activators of natural killer T cells as immunotherapeutic agents. *Clin Transl Immunology* **2016**, *5* (4), e69.
8. (a) Fujii, S.; Shimizu, K.; Kronenberg, M.; Steinman, R. M., Prolonged IFN-gamma-producing NKT response induced with alpha-galactosylceramide-loaded DCs. *Nature immunology* **2002**, *3* (9), 867-74; (b) Kimura, H.; Matsui, Y.; Ishikawa, A.; Nakajima, T.; Yoshino, M.; Sakairi, Y., Randomized controlled phase III trial of adjuvant chemo-immunotherapy with activated killer T cells and dendritic cells in patients with resected primary lung cancer. *Cancer Immunol Immunother* **2015**, *64* (1), 51-9; (c) Stirnemann, K.; Romero, J. F.; Baldi, L.; Robert, B.; Cesson, V.; Besra, G. S.; Zauderer, M.; Wurm, F.; Corradin, G.; Mach, J. P., et al., Sustained activation and tumor targeting of NKT cells using a CD1d-anti-HER2-scFv fusion protein induce antitumor effects in mice. *The Journal of clinical investigation* **2008**, *118* (3), 994-1005; (d) Cognac, S.; Perret, R.; Derre, L.; Zhang, L.; Stirnemann, K.; Zauderer, M.; Speiser, D. E.; Mach, J. P.; Romero, P.; Donda, A., CD1d-antibody fusion proteins target iNKT cells to the tumor and trigger long-term therapeutic responses. *Cancer Immunol Immunother* **2013**, *62* (4), 747-60.
9. Wolf, B. J.; Choi, J. E.; Exley, M. A., Novel Approaches to Exploiting Invariant NKT Cells in Cancer Immunotherapy. *Front Immunol* **2018**, *9*, 384.

- 1  
2  
3 10. Parekh, V. V.; Wilson, M. T.; Olivares-Villagomez, D.; Singh, A. K.; Wu, L.;  
4 Wang, C. R.; Joyce, S.; Van Kaer, L., Glycolipid antigen induces long-term natural killer  
5 T cell anergy in mice. *The Journal of clinical investigation* **2005**, *115* (9), 2572-83.
- 6 11. (a) Naidenko, O. V.; Maher, J. K.; Ernst, W. A.; Sakai, T.; Modlin, R. L.;  
7 Kronenberg, M., Binding and antigen presentation of ceramide-containing glycolipids by  
8 soluble mouse and human CD1d molecules. *J Exp Med* **1999**, *190* (8), 1069-80; (b)  
9 Sidobre, S.; Hammond, K. J.; Benazet-Sidobre, L.; Maltsev, S. D.; Richardson, S. K.;  
10 Ndonye, R. M.; Howell, A. R.; Sakai, T.; Besra, G. S.; Porcelli, S. A., et al., The T cell  
11 antigen receptor expressed by Valpha14i NKT cells has a unique mode of  
12 glycosphingolipid antigen recognition. *Proceedings of the National Academy of  
13 Sciences of the United States of America* **2004**, *101* (33), 12254-9; (c) van den Elzen,  
14 P.; Garg, S.; Leon, L.; Brigl, M.; Leadbetter, E. A.; Gumperz, J. E.; Dascher, C. C.;  
15 Cheng, T. Y.; Sacks, F. M.; Illarionov, P. A., et al., Apolipoprotein-mediated pathways of  
16 lipid antigen presentation. *Nature* **2005**, *437* (7060), 906-10; (d) Yuan, W.; Qi, X.;  
17 Tsang, P.; Kang, S. J.; Illarionov, P. A.; Besra, G. S.; Gumperz, J.; Cresswell, P.,  
18 Saposin B is the dominant saposin that facilitates lipid binding to human CD1d  
19 molecules. *Proceedings of the National Academy of Sciences of the United States of  
20 America* **2007**, *104* (13), 5551-6.
- 21 12. (a) Gao, B.; Radaeva, S.; Park, O., Liver natural killer and natural killer T cells:  
22 immunobiology and emerging roles in liver diseases. *Journal of leukocyte biology* **2009**,  
23 *86* (3), 513-28; (b) Szabo, P. A.; Rudak, P. T.; Choi, J.; Xu, S. X.; Schaub, R.; Singh, B.;  
24 McCormick, J. K.; Haeryfar, S. M. M., Invariant Natural Killer T Cells Are Pathogenic in  
25 the HLA-DR4-Transgenic Humanized Mouse Model of Toxic Shock Syndrome and Can  
26 Be Targeted to Reduce Morbidity. *J Infect Dis* **2017**, *215* (5), 824-829.
- 27 13. (a) Koch, M.; Stronge, V. S.; Shepherd, D.; Gadola, S. D.; Mathew, B.; Ritter, G.;  
28 Fersht, A. R.; Besra, G. S.; Schmidt, R. R.; Jones, E. Y., et al., The crystal structure of  
29 human CD1d with and without alpha-galactosylceramide. *Nature immunology* **2005**, *6*  
30 (8), 819-26; (b) Zeng, Z.; Castano, A. R.; Segelke, B. W.; Stura, E. A.; Peterson, P. A.;  
31 Wilson, I. A., Crystal structure of mouse CD1: An MHC-like fold with a large  
32 hydrophobic binding groove. *Science* **1997**, *277* (5324), 339-45.
- 33 14. Mitchell, D.; Lukeman, M.; Lehnher, D.; Wan, P., Formal intramolecular  
34 photoredox chemistry of meta-substituted benzophenones. *Org Lett* **2005**, *7* (15), 3387-  
35 9.
- 36 15. Im, J. S.; Arora, P.; Bricard, G.; Molano, A.; Venkataswamy, M. M.; Baine, I.;  
37 Jerud, E. S.; Goldberg, M. F.; Baena, A.; Yu, K. O., et al., Kinetics and cellular site of  
38 glycolipid loading control the outcome of natural killer T cell activation. *Immunity* **2009**,  
39 *30* (6), 888-98.
- 40 16. Bricard, G.; Venkataswamy, M. M.; Yu, K. O.; Im, J. S.; Ndonye, R. M.; Howell,  
41 A. R.; Veerapen, N.; Illarionov, P. A.; Besra, G. S.; Li, Q., et al., Alpha-  
42 galactosylceramide analogs with weak agonist activity for human iNKT cells define new  
43 candidate anti-inflammatory agents. *PLoS One* **2010**, *5* (12), e14374.
- 44 17. Jeon, J.; Kang, J. A.; Shim, H. E.; Nam, Y. R.; Yoon, S.; Kim, H. R.; Lee, D. E.;  
45 Park, S. H., Efficient method for iodine radioisotope labeling of cyclooctyne-containing  
46 molecules using strain-promoted copper-free click reaction. *Bioorg Med Chem* **2015**, *23*  
47 (13), 3303-8.

- 1  
2  
3 18. Yu, K. O.; Im, J. S.; Illarionov, P. A.; Ndonge, R. M.; Howell, A. R.; Besra, G. S.;  
4 Porcelli, S. A., Production and characterization of monoclonal antibodies against  
5 complexes of the NKT cell ligand alpha-galactosylceramide bound to mouse CD1d.  
6 *Journal of immunological methods* **2007**, *323* (1), 11-23.
- 7 19. Arora, P.; Baena, A.; Yu, K. O.; Saini, N. K.; Kharkwal, S. S.; Goldberg, M. F.;  
8 Kunnath-Velayudhan, S.; Carreno, L. J.; Venkataswamy, M. M.; Kim, J., et al., A single  
9 subset of dendritic cells controls the cytokine bias of natural killer T cell responses to  
10 diverse glycolipid antigens. *Immunity* **2014**, *40* (1), 105-16.
- 11 20. (a) Thakur, M. S.; Khurana, A.; Kronenberg, M.; Howell, A. R., Synthesis of a 2"-  
12 deoxy-beta-GalCer. *Molecules* **2014**, *19* (7), 10090-102; (b) Arora, P.; Kharkwal, S. S.;  
13 Ng, T. W.; Kunnath-Velayudhan, S.; Saini, N. K.; Johndrow, C. T.; Chang, Y. T.; Besra,  
14 G. S.; Porcelli, S. A., Endocytic pH regulates cell surface localization of glycolipid  
15 antigen loaded CD1d complexes. *Chemistry and physics of lipids* **2015**, *191*, 75-83; (c)  
16 Huang, J. R.; Tsai, Y. C.; Chang, Y. J.; Wu, J. C.; Hung, J. T.; Lin, K. H.; Wong, C. H.;  
17 Yu, A. L., alpha-Galactosylceramide but not phenyl-glycolipids induced NKT cell anergy  
18 and IL-33-mediated myeloid-derived suppressor cell accumulation via upregulation of  
19 *egr2/3*. *Journal of immunology* **2014**, *192* (4), 1972-81.
- 20 21. Wingender, G.; Birkholz, A. M.; Sag, D.; Farber, E.; Chitale, S.; Howell, A. R.;  
21 Kronenberg, M., Selective Conditions Are Required for the Induction of Invariant NKT  
22 Cell Hyporesponsiveness by Antigenic Stimulation. *J Immunol* **2015**, *195* (8), 3838-48.
- 23 22. Giaccone, G.; Punt, C. J.; Ando, Y.; Ruijter, R.; Nishi, N.; Peters, M.; von  
24 Blomberg, B. M.; Scheper, R. J.; van der Vliet, H. J.; van den Eertwegh, A. J., et al., A  
25 phase I study of the natural killer T-cell ligand alpha-galactosylceramide (KRN7000) in  
26 patients with solid tumors. *Clinical cancer research : an official journal of the American  
27 Association for Cancer Research* **2002**, *8* (12), 3702-9.
- 28 23. (a) Ishikawa, A.; Motohashi, S.; Ishikawa, E.; Fuchida, H.; Higashino, K.; Otsuji,  
29 M.; Iizasa, T.; Nakayama, T.; Taniguchi, M.; Fujisawa, T., A phase I study of alpha-  
30 galactosylceramide (KRN7000)-pulsed dendritic cells in patients with advanced and  
31 recurrent non-small cell lung cancer. *Clinical cancer research : an official journal of the  
32 American Association for Cancer Research* **2005**, *11* (5), 1910-7; (b) Kunii, N.;  
33 Horiguchi, S.; Motohashi, S.; Yamamoto, H.; Ueno, N.; Yamamoto, S.; Sakurai, D.;  
34 Taniguchi, M.; Nakayama, T.; Okamoto, Y., Combination therapy of in vitro-expanded  
35 natural killer T cells and alpha-galactosylceramide-pulsed antigen-presenting cells in  
36 patients with recurrent head and neck carcinoma. *Cancer science* **2009**, *100* (6), 1092-  
37 8.
- 38 24. (a) Schmieg, J.; Yang, G.; Franck, R. W.; Tsuji, M., Superior protection against  
39 malaria and melanoma metastases by a C-glycoside analogue of the natural killer T cell  
40 ligand [alpha]-galactosylceramide. *J. Exp. Med.* **2003**, *198*, 1631-1641; (b) Aspeslagh,  
41 S.; Nemcovic, M.; Pauwels, N.; Venken, K.; Wang, J.; Van Calenbergh, S.; Zajonc, D.  
42 M.; Elewaut, D., Enhanced TCR footprint by a novel glycolipid increases NKT-  
43 dependent tumor protection. *Journal of immunology* **2013**, *191* (6), 2916-25.
- 44 25. Girardi, E.; Yu, E. D.; Li, Y.; Tarumoto, N.; Pei, B.; Wang, J.; Illarionov, P.; Kinjo,  
45 Y.; Kronenberg, M.; Zajonc, D. M., Unique interplay between sugar and lipid in  
determining the antigenic potency of bacterial antigens for NKT cells. *PLoS Biol* **2011**, *9*  
(11), e1001189.

- 1  
2  
3 1 26. Exley, M.; Garcia, J.; Balk, S. P.; Porcelli, S., Requirements for CD1d recognition  
4 2 by human invariant Valpha24+ CD4-CD8- T cells. *J Exp Med* **1997**, *186* (1), 109-20.  
5 3 27. Khurana, A.; Kronenberg, M., A method for production of recombinant mCD1d  
6 4 protein in insect cells. *J Vis Exp* **2007**, (10), 556.  
7 5 28. Im, J. S.; Yu, K. O.; Illarionov, P. A.; LeClair, K. P.; Storey, J. R.; Kennedy, M.  
8 6 W.; Besra, G. S.; Porcelli, S. A., Direct measurement of antigen binding properties of  
9 7 CD1 proteins using fluorescent lipid probes. *The Journal of biological chemistry* **2004**,  
10 8 *279* (1), 299-310.  
11 9 29. Arora, P.; Venkataswamy, M. M.; Baena, A.; Bricard, G.; Li, Q.; Veerapen, N.;  
12 10 Ndonye, R.; Park, J. J.; Lee, J. H.; Seo, K. C., et al., A rapid fluorescence-based assay  
13 11 for classification of iNKT cell activating glycolipids. *Journal of the American Chemical*  
14 12 *Society* **2011**, *133* (14), 5198-201.  
15 13 30. Jervis, P. J.; Veerapen, N.; Bricard, G.; Cox, L. R.; Porcelli, S. A.; Besra, G. S.,  
16 14 Synthesis and biological activity of alpha-glucosyl C24:0 and C20:2 ceramides. *Bioorg*  
17 15 *Med Chem Lett* **2010**, *20* (12), 3475-8.

16

17

18

19

20

21

22

23

24

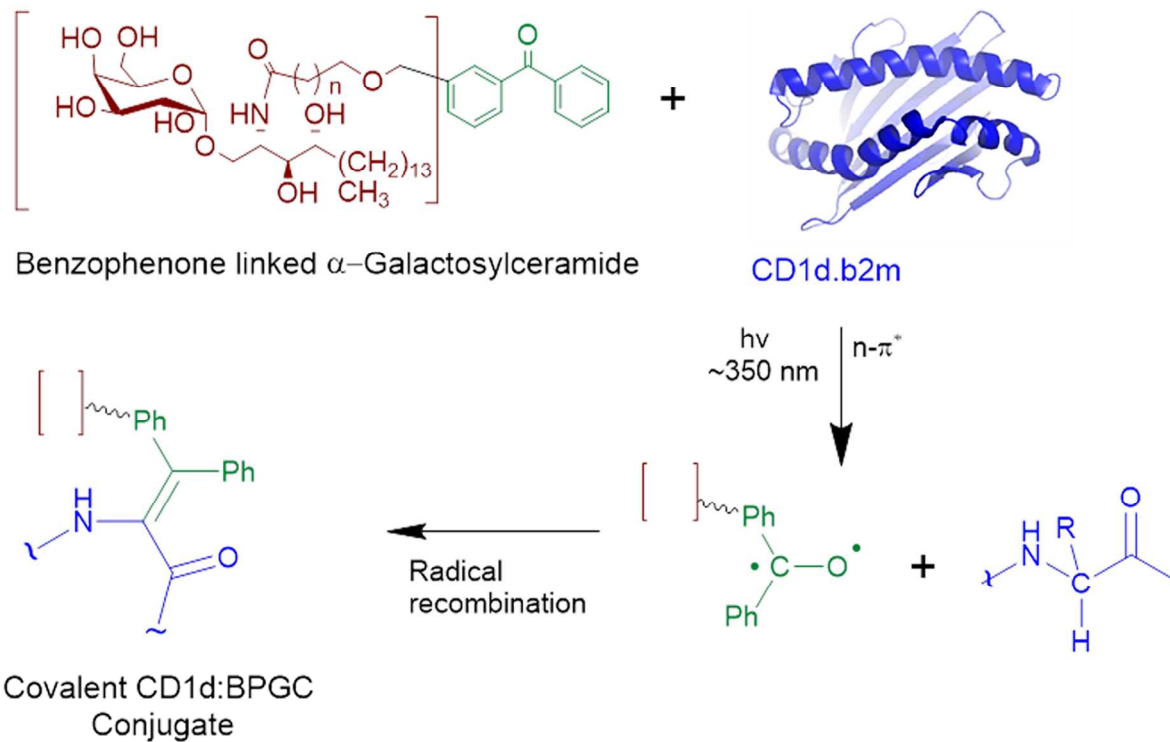
25

26

27

1

2 For Table of Contents Only



3